

The decay of multiscale signals – deterministic model of the Burgers turbulence

S.N. Gurbatov^{1,3}, A.V. Trousov^{2,3}

October 29, 2018

- ¹ Radiophysics Dept., University of Nizhny Novgorod
23, Gagarin Ave., Nizhny Novgorod 603600, Russia.
E-mail: gurb@rf.unn.runnet.ru
(Permanent address)
- ² Joint Institute of Physics of the Earth RAS,
Molodezhnaya Str., 3, GC RAS, Moscow, 117296 Russia.
E-mail: shtrssv@cityline.ru, troussov@hotmail.com
(Permanent address)
- ³ Observatoire de la Cote d’Azur, Laboratoire G.D. Cassini,
B.P. 229, 06304, Nice Cedex 4, France.

Corresponding author: 3731007. Sergey N. Gurbatov, Radiophysics Dept.,
University of Nizhny Novgorod, 23, Gagarin Ave., Nizhny Novgorod 603600, Russia.
E-mail: gurb@rf.unn.runnet.ru.
Tel.: (8 312) 656002, Fax: (8 312) 656416,
Tel.(Home): (8 312) 340969.

Abstract

This work is devoted to the study of the decay of multiscale deterministic solutions of the unforced Burgers’ equation in the limit of vanishing viscosity.

It is well known that Burgers turbulence with a power law energy spectrum $E_0(k) \sim |k|^n$ has a self-similar regime of evolution. For $n < 1$ this regime is characterised by an integral scale $L(t) \sim t^{2/(3+n)}$, which increases with the time due to the multiple mergings of the shocks, and therefore, the energy of a random wave decays more slowly than the energy of a periodic signal.

In this paper a deterministic model of turbulence-like evolution is considered. We construct the initial perturbation as a piecewise linear analog of the Weierstrass function. The wavenumbers of this function form a "Weierstrass spectrum", which accumulates at the origin in geometric progression. "Reverse" sawtooth functions with negative initial slope are used in this series as basic functions, while their amplitudes are chosen by the condition that the distribution of energy over exponential intervals of wavenumbers is the same as for the continuous spectrum in Burgers turbulence. Combining these two ideas allows us to obtain an exact analytical solution for the

velocity field. We also notice that such multiscale waves may be constructed for multidimensional Burgers' equation.

This solution has scaling exponent $h = -(1+n)/2$ and its evolution in time is self-similar with logarithmic periodicity and with the same average law $L(t)$ as for Burgers turbulence. Shocklines form self-similar regular tree-like structures. This model also describes important properties of the Burgers turbulence such as the self-preservation of the evolution of large scale structures in the presence of small scales perturbations.

PACS 43.25.Cb,47.27.Eq.

Keywords: Burgers' equation; Burgers turbulence

1 Introduction

The nonlinear diffusion equation

$$\frac{\partial v}{\partial t} + v \frac{\partial v}{\partial x} = \nu \frac{\partial^2 v}{\partial x^2}; \quad v(x, t = 0) = v_0(x). \quad (1.1)$$

was originally introduced by J.M.Burgers in [6] (1939) as a model for hydrodynamical turbulence. Burgers' equation (1.1) describes two fundamental effects characteristic of any turbulence [10]: the nonlinear redistribution of energy over the spectrum and the action of viscosity in small scales. Burgers' equation was used later to describe a large class of physical systems in which the nonlinearity is fairly weak (quadratic) and the dispersion is negligible compared to the linear damping [29]. The most important example of such waves are acoustical waves with finite amplitude [24]. Another class of problems, arising, e.g., in surface growth, also leads to Burgers' equation [5],[8],[30]. The three dimensional form of (1.1) has been used in cosmology to describe the formation of large scale structures of the Universe at a nonlinear stage of gravitational instability (see e.g. [15], [25], [13], [28]).

In the physically important case of large Reynolds number, the action of viscosity is significant only in the small regions with high gradient of the velocity field. In the limit $\nu \rightarrow 0$, the solution of Burgers' equation has the following form (see [18], [7], [13]):

$$v(x, t) = \frac{x - y(x, t)}{t}, \quad (1.2)$$

where $y(x, t)$ is the coordinate of the maximum of the function

$$G(x, y, t) = \Psi_0(y) - \frac{(x - y)^2}{2t}, \quad v_0(x) = -\frac{\partial \Psi_0(x)}{\partial x}. \quad (1.3)$$

Strong interaction between coherent harmonics leads to the appearance of local self-similar structures in Burgers' equation. A periodic initial perturbation with zero mean velocity is transformed asymptotically into a sawtooth wave with gradient $\partial_x v = 1/t$ and with the same period l_0 . It is important that at this stage the amplitude $a(t) = l_0/t$ and the energy density $\sigma^2(t) \simeq l_0^2/12t^2$ do not depend on the initial amplitude.

An initial one-signed pulse with the area $m > 0$, localised at $t = 0$ in the neighbourhood of the point $x = 0$, also has asymptotically a universal form: it transforms into a triangular pulse with the gradient $\partial_x v = 1/t$ and increasing coordinate of the shock $x_s \approx (2mt)^{1/2}$. Due to the increase of the integral scale the amplitude of such a pulse $a(t) = x_s(t)/t \sim m^{1/2}t^{-1/2}$ and its energy will decrease more slowly than for a periodic signal, like $t^{-1/2}$.

Continuous random initial fields are also transformed into sequences of regions with the same gradient $\partial_x v = 1/t$, but with random locations of the shocks separating them. Due to the multiple merging of the shocks the statistical properties of such random fields are also self-similar and may be characterised by the integral scale of the turbulence $L(t)$. The merging of the shocks leads to an increase of the integral scale $L(t)$, and because of this the energy

$$\sigma^2(t) \sim L^2(t)/t^2 \quad (1.4)$$

of a random wave decreases more slowly than the energy of periodic signals.

The type of turbulence evolution is determined by the behaviour of the large scale part of the initial energy spectrum

$$E_0(k) = \alpha^2 k^n b_0(k); \quad (1.5)$$

$$E_0(k) = \frac{1}{2\pi} \int \langle v_0(x), v_0(x+z) \rangle e^{ikz} dz. \quad (1.6)$$

Here $b_0(k)$ is a function which falls off rapidly for $k > k_0 \sim l_0$, and $b_0(0) = 1$. For $n > 1$ the law of energy decay strongly depends on the statistical properties of the initial field (see e.g. [30] and references therein). For the initial Gaussian perturbation the integral scale $L(t) \sim t^{1/2}$ times logarithmic correction obtains and is determined by two integral characteristics of the initial spectrum: the variances of the initial potential Ψ_0 and the velocity $v_0(x)$ [20],[9],[13],[16].

For $n < 1$ the structure function of the initial potential increases as a power law in space. Then the initial potential field is Brownian, or fractional Brownian motion, and some scaling may be used [7],[20], [13], [26], [3],[22], [23]. In this case the turbulence is also self-similar and the integral scale $L(t)$ increases as

$$L(t) = (\alpha t)^{2/(3+n)}. \quad (1.7)$$

The energy of the turbulence is derived from (1.4):

$$\sigma^2(t) \sim t^{-p}, \quad p = \frac{2(n+1)}{n+3}. \quad (1.8)$$

The difference between these two cases ($n < 1$ and $n > 1$) is connected to the process of parametric generation of low frequency component of the spectrum. For the case $n < 1$ the newly generated low frequency components are relatively small and we have the conservation of large scale part of the spectrum:

$$E(k, t) = E_0(k) = \alpha^2 k^n, \quad \text{for } k \ll 1/L(t). \quad (1.9)$$

Thus, the laws of turbulent decay are more complex than for simple signals, which can be attributed to multiple merging of the shocks. In [12] a model of a regular fractal signal

with decay lower than for single one-signed pulse was introduced. The initial signal $v_0(x)$ was constructed as a sequence of one-signed pulses whose positions form a Cantor set with capacity (fractal dimension) $D = \ln N / \ln \beta$, where N^p is the number of pulses in the scale $L_p \simeq L_1 N \beta^{p-1}$, $0 < D < 1$. Multiple merging makes the decay of the wave slower and the general behaviour of the energy decay may be approximated by the power law with the exponent in (1.8):

$$p = \frac{1 - D}{2 - D}, \quad 0 < p < 1. \quad (1.10)$$

The evolution proves to be self-similar in successive time periods (t_i, t_{i-1}) and (t_{i+1}, t_{i+2}) , where $t_{i+1}/t_i = \beta^2/N$. This shows log-periodical self-similarity of the field evolution. Linear and non-linear decay of fractal and spiral fields given by the sequences of regular pulses was also investigated in [1]. It was shown that the power law (1.8) with the exponent given by the formula (1.10) holds also true for homogeneous fractal pulse signal with capacity D .

Another model of a multiscale signal, which has the same general behaviour on the external scale $L(t)$ (1.7), and energy of the Burgers turbulence, was also discussed in [12]. It was assumed therein that the initial signal is a discrete set of modes - the spatial harmonics

$$v_0(x) = \sum_{p=0}^{\infty} a_p \sin(k_p x + \varphi_p), \quad (1.11)$$

with wavenumbers k_p and amplitudes a_p given in terms of a parameter ϵ by

$$\begin{aligned} k_p &= k_0 \epsilon^p, & a_p &= a_0 \epsilon^{-hp}, \\ h &= -\left(\frac{n+1}{2}\right), & a_0 &= \alpha k_0^{(n+1)/2}. \end{aligned} \quad (1.12)$$

Amplitudes a_p and the scaling exponent h are chosen from the condition that the mean energy of harmonics in the interval $\Delta_p = k_p - k_{p+1}$ be identical to that corresponding to the spectral density (1.5): $a_p^2 = E(k_p) \Delta_p$. For $\epsilon \ll 1$ and $n > -1$ the harmonics are spread over the spatial spectrum and accumulate at the point $k = 0$ with decreasing amplitude. The main approach in this model was that the energy of the wave is the sum of energies of independent modes. The approach is nontrivial, but nevertheless leads to the same laws of the integral scale $L(t)$ (1.7) and the energy decay (1.8) as in the case of continuous spectrum (1.5). Let us point out that representation of the field given by the formula (1.11) is similar to shell models, which were introduced as useful models addressing the problem of analogous scaling in fully developed turbulence (see, e.g., [11], [19] and references in there).

In present paper we consider the evolution of a regular signal whose behaviour in general is similar to the evolution of the Burgers turbulence with continuous spectrum (1.5). The main difference, as compared to the model discussed above, is that we construct the exact solution of Burgers' equation using as an initial mode the "reverse" sawtooth wave. The frequency ratio in our model is $\epsilon = 1/N$, where N is an integer and $N \geq 2$. These perturbations are similar to the well known Weierstrass and Weierstrass-Mandelbrot fractal functions (see [21], [4]).

For the analysis of Burgers' equation it is convenient to use a mechanical interpretation. There is a one-to-one correspondence between the solution of Burgers' equation and the

dynamic of a gas of inelastically interacting particles [13], [14]. Let us take a one-dimensional particle flux with a contact interaction: as long as the particles do not run into each other they move with constant velocity. In the collision they stick together, forming a delta-function singularity in the matter density. This leads to the appearance of gas of two species: a hydrodynamical flux of the "light" initial particles, and a gas of "heavy" particles arising in the adhesion process of light particles. The evolution of the particle velocity field will be described by the solution of Burgers' equation if we assume that the initial density of the light particles is $\rho_0 = const$, the velocity of particles is equal to the initial velocity in (1.1), and that the collision of the particles conserve their mass and momentum. This analogy permits construction of a very fast (linear time) algorithm of solution of Burgers' equation [27].

In our case, for the initial reverse sawtooth wave, all the matter turns into heavy particles at the same moment of time. Thus, after this time the evolution of the Burgers turbulence is fully determined by the motion of heavy particles, whose positions are positions of shocks, and masses are equal to $\Delta v \cdot t$, where Δv are the amplitudes of the shocks.

The paper is organized as follows. In Section 2 we consider the evolution and interaction of "reverse" sawtooth modes. In section 3 we consider the interaction of small scale mode with large scale structures. In Section 4 we investigate the properties of the sawtooth Weierstrass-Mandelbrot fractal function. In section 5 we show that deterministic model has logarithmic periodic self-similarity. We also discuss here the multi-dimensional generalization of this model. Section 5 presents concluding remarks.

2 Evolution and interaction of "reverse" sawtooth modes in Burgers' equation

Let us introduce the p th "reverse" saw tooth mode as

$$v_{(p)}(x, 0) = a_p A(k_p x + \varphi_p) \quad (2.1)$$

Here a_p, k_p are amplitude and wavenumber of the mode, $-\varphi_p$ is its phase. The function $A(x)$ is 2π periodic function, given on its first period by the following expression

$$A(x) = \pi - x, \quad x \in [0, 2\pi[\quad (2.2)$$

The set of "reverse sawtooth" functions is not orthogonal, but nevertheless we will introduce a set of modes satisfying equation (1.12), whose wavenumbers and amplitudes satisfy the same relations as the sinusoidal modes of [12], i.e. relation (1.11). We introduce the term "reverse sawtooth" because this signal is a sawtooth with teeth facing to the right, but the term "sawtooth" by itself is widely used in Burgers turbulence literature to refer to the late stage of the evolution of the wave profile a sequence of sawteeth with *positive* slope $1/t$.

The solution of Burgers' equation with a linear velocity profile $v_0 = -\gamma(x - x_+)$ is well-known (see, e.g., [13]):

$$v(x, t) = \frac{-\gamma(x - x_+)}{1 - \gamma t} \quad (2.3)$$

The value γ^{-1} has the dimension of time, and for $\gamma > 0$, at the finite time $t = \gamma^{-1}$ the gradient $\partial_x v$ becomes infinite. For $\gamma < 0$ the gradient becomes equal to $\partial_x v = t^{-1}$, independent of the value of γ at times $t \gg |\gamma|^{-1}$. Thus, we have from (1.12), (2.1),(2.2), that the evolution of the p th mode is characterised by the nonlinear time

$$t_p = \gamma_p^{-1} = a_p k_p^{-1} = t_0 / (\epsilon^{(n+3)/2})^p, \quad t_0 = 1 / \alpha k_0^{n+3/2} \quad (2.4)$$

Based on solution (2.3) it is easy to see that for the "first" period (if $\varphi_p = 0$) the evolution of the p th reverse mode at the initial stage ($t < t_p$) may be described as

$$v_{(p)}(x, t) = \begin{cases} x/t, & \text{if } 0 < x < \frac{t}{t_p} \frac{\pi}{k_p}; \\ \frac{1}{t_p} \left(\frac{\pi}{k_p} - x \right) / \frac{1}{1-t/t_p}, & \text{if } \left| \frac{\pi}{k_p} - x \right| < \frac{t}{t_p} \frac{\pi}{k_p}; \\ (x - \frac{\pi}{k_p})/t, & \text{if } \frac{t}{t_p} \frac{\pi}{k_p} < x - \frac{\pi}{k_p} < \frac{\pi}{k_p}. \end{cases} \quad (2.5)$$

On the other hand, at time $t = t_p$, the mode transforms into a "direct" sawtooth wave with slope $\partial_x v = 1/t$, independent of the amplitude and wavenumber of the mode:

$$v_{(p)}(x, t) = \begin{cases} x/t, & \text{if } 0 < x < \frac{\pi}{k_p}; \\ (x - \frac{\pi}{k_p})/t, & \text{if } \frac{\pi}{k_p} < x < \frac{2\pi}{k_p}. \end{cases} \quad (2.6)$$

The density of energy $\sigma^2(t) = \langle v^2(x, t) \rangle_L$, where $\langle \rangle_L$ denotes averaging over the period, is conserved before $t < t_p$, and decreases like $(k_p t)^{-2}$ after $t > t_p$.

Consider now the evolution of a gas of sticky particles in the case of independent evolution of the p th mode. In the general case, the density of the gas is calculated by using the Jacobian of the transformation from Lagrangian to Eulerian coordinates and may be written in the form (see, e.g., [13])

$$\rho(x, t) = \rho_0 (1 - t \partial_x v(x, t)) \quad (2.7)$$

Then it is obvious that at the initial stage

$$\rho(x, t) = \rho_0 \frac{1}{1 - t/t_p}, \quad \left| \frac{\pi}{k_p} - x \right| < \frac{t}{t_p} \frac{\pi}{k_p} \quad (2.8)$$

while ρ is zero outside this interval in each period. At time $t = t_p$ all the light particles in each period collide into a single heavy particle with mass

$$m_p = \rho_0 L_p = \rho_0 \frac{2\pi}{k_p}, \quad (2.9)$$

and the heavy particles have positions

$$x_{p,l} = \frac{\pi}{k_p} - \frac{\varphi_p}{k_p} + \frac{2\pi}{k_p} l; \quad l = 0, \pm 1, \pm 2, \dots \quad (2.10)$$

equal to the zero positions of the initial p th mode. The process of light merging particles and the evolution of the velocity is shown in Fig.1.

Consider now the joint evolution of two successive modes: p th and $(p+1)$ th. From (2.4) one can see that the ratio of nonlinear times of the successive modes is

$$\frac{t_{p+1}}{t_p} = \epsilon^{-(n+3)/2} \equiv \epsilon^{1-h}, \quad (2.11)$$

which does not depend on p and increases if the exponent n is greater than -3 . The gradient of the initial field $v_{(p)}(x) + v_{(p+1)}(x)$ is $-(\gamma_p + \gamma_{p+1})$, so the effective nonlinear time for such a sum is

$$t_{p,eff} = t_{p,p+1} = \frac{1}{\gamma_p + \gamma_{p+1}} = \frac{t_p}{1 + t_p/t_{p+1}}, \quad (2.12)$$

Because all parts of the initial perturbation have the same slope, all light particles will collide at the same time $t = t_{p,p+1}$.

The mass of heavy particles after merging are $m_{p,i} = \rho_0 \Delta_{i,i+1}$, where $\Delta_{i,i+1}$ is the distance between adjacent shocks in the initial perturbation. The ratio of periods of two adjacent modes is $L_{p+1}/L_p = k_p/k_{p+1} = \epsilon^{-1}$. If $N = \epsilon^{-1}$ is an integer larger than 1, there will be $N+1$ heavy particles on the period of the larger scale mode $(p+1)$ th: $(N-1)$ with the mass $m_p = \rho_0 L_p$ (2.9), and two particles with total mass equal to m_p . These two particles only exist when the shock of the $(p+1)$ th mode is located in the interval between shocks of the p th mode. For simplicity, we will consider the case where the spatial relations

$$k_{p+1}\varphi_{p+1} = k_p\varphi_p + 2\pi r/N, \quad (2.13)$$

between the phases of successive modes, hold. In this case the discontinuities of the $(p+1)$ th mode do not produce new shocks in the total perturbation $v_{(p)}(x) + v_{(p+1)}(x)$. Thus, at times t larger than $t > t_{r,eff}$, the masses of all heavy particles will be the same, as would be the case without the large scale modes (2.9).

The positions of these heavy particles at time $t = t_{p,eff}$ are

$$X_{(p,l)}(t_{p,eff}) = x_{p,l} + v_{(p+1)}(x_{p,l})t_{p,eff}, \quad (2.14)$$

where $x_{p,l}$ are the zero positions of the p th mode (2.10). The velocity of this particle is equal to $v_{(p+1)}(x_{p,l})$. Equation (2.14) is obvious if we use the trivial equality $v_{(p)}(x_{p,l}) + v_{(p+1)}(x_{p,l}) = v_{(p+1)}(x_{p,l})$, and also note that the position of the heavy particle $x_{p,l}(t_{p,eff})$ is equal to the position at the same time of all light particles with initial coordinate $x = x_{p,l}$. From (2.14) we immediately have that after time $t_{p,eff}$ the positions of the particles are

$$X_{(p,l)}(t) = x_{p,l} + v_{(p+1)}(x_{p,l})t. \quad (2.15)$$

The difference between the coordinates of the adjacent particles $X_{p,l}(t)$ and $X_{p,l+1}(t)$ decreases with time, proportionally to the gradient of $v_{(p+1)}(x)$:

$$\begin{aligned} X_{(p,l+1)}(t) - X_{p,l}(t) &= (x_{p,l+1} - x_{p,l}) - t \frac{\partial v_{(p+1)}(x)}{\partial x} (x_{p,l+1} - x_{p,l}) \equiv \\ &= (x_{p,l+1} - x_{p,l})(1 - t/t_{p+1}). \end{aligned} \quad (2.16)$$

These particles collide at time $t = t_{p+1}$ (2.4) and the newly created heavy particles will have masses

$$m_{(p+1)} = \rho_0 L_{p+1} \quad (2.17)$$

and positions

$$x_{p+1,l} = \frac{\pi}{k_{p+1}} - \frac{\varphi_{p+1}}{k_p} + \frac{2\pi l}{k_{p+1}}; \quad l = 0, \pm 1, \pm 2, \dots \quad (2.18)$$

The velocity of these particles is zero.

Thus, at times t larger than t_{p+1} , the evolution of the initial perturbation $v_0(x) = v_{(p)}(x) + v_{(p+1)}(x)$ will be the same as the evolution of only the large scale mode $v_{(p+1)}(x)$. The process of particles merging and the evolution of the velocity for the sum of two successive modes with the periods ratio $N = 2$ are shown in Fig. 2.

By recurrence, it is evident that for finite number of modes $v(x) = v_{(p)}(x) + v_{(p+1)}(x) + \dots + v_{(M)}(x)$ the evolution of the field after t_M will be the same as the evolution of only the largest mode $v_{(M)}(x)$. The reason for this, is of course, the special relation between the phases φ_p and the wavenumbers k_p of all interacting modes: $k_p = k_0/N^p$ (see equation (1.12)). For integer N the minimal value of any combination of these wavenumbers is equal to the largest mode wavenumber $k_M = k_0/N^M$. So the nonlinear interaction does not produce new components at frequencies less than k_M .

3 Interaction of small scale "reverse" sawtooth mode with large scale structures

Let us now consider the interaction of the p th mode with an infinite series of larger scale modes

$$W_p(x) = \sum_{r=p+1}^{\infty} v_r(x) \equiv \sum_{r=p+1}^{\infty} a_r A(k_r x + \varphi_r), \quad (3.1)$$

assuming that the phases of the modes satisfy the relations (2.13) and that $k_r = k_0 \epsilon^r$, $a_r = a_0 \epsilon^{-hr}$, $h = -(n+1)/2$. From (3.1) and (2.4) we have for the gradient of the initial perturbation $v_0(x) = v_p(x) + W_p(x)$

$$\begin{aligned} \partial_x v_0(x) &= \partial_x v_p(x) + \partial_x W_p(x) = \sum_{r=p}^{\infty} \gamma_r = \\ &= \gamma_0 \sum_{r=p}^{\infty} (\epsilon^{\frac{(n+3)}{2}})^r = \gamma_0 \epsilon^{\frac{(n+3)}{2}p} \frac{1}{1 - \epsilon^{\frac{(n+3)}{2}}}, \end{aligned} \quad (3.2)$$

the condition $n > -3$ ($h < 1$) being necessary for the series to converge. From (3.2), we have for the effective time of nonlinearity of p th mode

$$\tilde{t}_p = 1/\partial_x v_0(x) = t_p (1 - \epsilon^{\frac{(n+3)}{2}}), \quad (3.3)$$

with the original t_p determined by the equation (2.4).

Thus, after the time of collision \tilde{t}_p , heavy particles with mass $m_p = \rho_0 L_p$ (3.2) appear. The coordinates of these particles will be determined by an equation similar to (2.15)

$$x_{p,l}(t) = x_{p,l}(\tilde{t}_p) + W_p(x_{p,l})t, \quad (3.4)$$

with the velocity of particles determined by the function $W_p(x)$ (see 3.1), which is a sum of all larger modes, and $x_{p,l}$ are the coordinates of the zeros of the p th modes. The difference between the coordinates of adjacent particles $x_{p,l}$ and $x_{p,l+1}$ will then decrease with time like $(1 - t/\tilde{t}_{p+1})$, where $\tilde{t}_{p+1} = t_{p+1}(1 - \epsilon^{(n+3)/2})$ is the inverse of the gradient of the function $W_p(x)$, see (3.1) and (3.2). Thus, the time of particle collision for this generation will be described by equation (3.3) with $p = p + 1$, and the new masses will be determined by the period of the $(p + 1)$ th mode - see equation (2.17).

The extrapolation of this particle merging process to the next generations is evident by recurrence. The q th collision of heavy particles takes place at time $\tilde{t}_{p+q} = t_{p+q}(1 - \epsilon^{\frac{n+3}{2}})$, the masses of these particles at this time are determined by the period of the $(p + q)$ th mode $m_{p+q} = \rho_0 L_{p+q} = 2\pi\rho_0/k_{p+q}$ (2.9), (2.17). In the time interval $t \in [\tilde{t}_{p+q}, \tilde{t}_{p+q+1}]$,

$$\frac{\tilde{t}_{p+q+1}}{\tilde{t}_{p+q}} = \epsilon^{-\frac{(n+3)}{2}} = N^{\frac{n+3}{2}}; \quad (3.5)$$

the coordinates of particles will be determined by the equation (3.4) with $p = p + q$. Here $W_{p+q}(x)$ is the sum of the velocities of all larger modes with $r > p + q$, and $x_{p+q,l}$ are the zeros of $(p + q)$ -th mode. It is important to note that at time $t > \tilde{t}_{p+q}$ the evolution of the particles is solely determined by the modes with $r \geq p + q$. It means, that at times $t > \tilde{t}_{p+q}$ the position of the particles does not depend on the presence in the initial condition of the small scale modes with $r < p + q$.

Thus, two processes with different initial velocities: $\tilde{v}_0(x)$, the field with small scales, and $v_0(x)$, the field without small scales modes:

$$v_0(x) = W_{p+q-1}(x); \quad \tilde{v}_0(x) = W_{p-1}(x) \quad (3.6)$$

will have the same evolution after $t > \tilde{t}_{p+q-1}$. Even if $p \rightarrow -\infty$ (when modes with very small scales $L_p \sim \epsilon^{-p} = N^p$ and very large amplitudes $a_p \sim a_0(\epsilon^{(n+1)/2})^p = a_0(N^{(n+1)/2})^{-p}$ are present in the initial perturbation) the multiple merging of the particles will lead to the independence of the evolution of large scale modes with respect to the small scale modes.

This effect is similar to the self-preservation of large scale structures in Burgers turbulence [2],[17]. When the initial field $v_0(x)$ is noise, the highly nonlinear structures continuously interact and due to the merging of shocks, their characteristic scale $L(t)$ constantly increases. The presence of small scale noise perturbation $v_h(x)$ results in additional fluctuations in the shock coordinates $\Delta x_k(t)$, and these fluctuations increase in strength with the passage of time. Thus, the final result of the evolution of the field is determined by the competition of two factors, the increase in the external scale $L(t)$ of the structures and the increase in the strength $\Delta x_k(t)$ of shock coordinates fluctuations, the later being related to the perturbation $v_h(x)$. In a turbulence, having power index $n < 1$ (1.5), multiple merging of shocks leads to self-preservation of the large scale structures independently of the presence

of small scale components. For the model signal this effect appears for arbitrary n due to the special choice of wavenumbers and phases of interacting modes.

It was stressed in the introduction that the solution of Burgers' equation has a one-to-one correspondence with the dynamics of the gas of inelastically interacting particles ([13]). The stage when all light particles collide, forming heavy particles, corresponds to the solution of Burgers' equation with a well-defined slope $\partial_x v = 1/t$. In this case the profile of the field $v(x, t)$ is fully determined by the coordinates and amplitudes of the shocks. Their coordinates $X_s(t)$ are equal to the coordinates of heavy particles, their velocity

$$v_s(t) = \frac{dX_s(t)}{dt} = (v_s(x_s - 0, t) + v_s(x_s + 0, t))/2 \quad (3.7)$$

is equal to the velocity of the particles, and the amplitude of the shock

$$\Delta v_s(x) = (v(x_s - 0, t) - v(x_s + 0, t)) = m/t \quad (3.8)$$

is determined by the mass of the particle ($\rho_0 \equiv 1$) (see, e.g., [13]).

Thus, the investigation of the motion of heavy particles permits to fully reconstruct the properties of the velocity field $v(x, t)$ of Burgers' equation.

4 The sawtooth Weierstrass-Mandelbrot fractal function

It was shown in the previous section that the evolution of the particles (shocks) is determined by the function $W_p(x)$ (3.1). The basis functions of $W_p(x)$ are the reverse sawtooth periodic functions with wavenumbers $k_r = k_0 \epsilon^r$ and amplitudes $a_r = a_0 \epsilon^{-hr}$, $h = -(n+1)/2$ satisfy relations (1.12). Wavenumbers form a geometrical progression like in the Weierstrass function (see [4]) and accumulate at the origin $k = 0$. In the original Weierstrass function, the situation was the opposite with increasing frequencies, but nevertheless the function $W_p(x)$ has many properties of Weierstrass function and of its generalisation – the Weierstrass-Mandelbrot function (see [21], [4]).

We consider here a deterministic function $W_p(x)$ with the special phase relation $\varphi_p = (2\pi k/N)p$ ($k = 1, 2, \dots, N; N = 1/\epsilon$), thus, the discontinuities in the largest modes $r > p + 1$ coincide with some of the discontinuities of the smaller mode $r = p + 1$. The function $W_p(x)$ is continuous in the intervals $2\pi/k_{p+1} = 2\pi/(k_0 \epsilon^{p+1})$ with the same slope in each interval. The inverse value of this slope \tilde{t}_{p+1}

$$\tilde{t}_{p+1} = t_{p+1}(1 - \epsilon^{\frac{n+3}{2}}); \quad t_{p+1} = t_0(\epsilon^{\frac{n+3}{2}})^{p+1} \quad (4.1)$$

is proportional to the nonlinear time t_{p+1} of the smallest mode. Of course, we need $n > -3$, so that the convergence of (3.2) is assured and the inequalities $t_{p+1} > t_p$ hold. The amplitudes of the modes are proportional to $\epsilon^{(n+1)/2}$ and for $n > -1$ the function $W_p(x)$ is bounded

$$W_p(x) \leq \sum_{r=p+1}^{\infty} a_r = a_0(\epsilon^{\frac{n+1}{2}})^{p+1} \frac{1}{1 - \epsilon^{\frac{n+1}{2}}} \quad (4.2)$$

Thus, for finite p the energy of $W_p(x)$ is also finite. For the case of the phase relation introduced above, the functions $W_p(x)$ also have scaling properties, so that for instance for $k = 0$, we have

$$W_p(\tilde{x}) = \epsilon^{-hp}W_0(\epsilon^p x); \quad W_p(\epsilon^m x) = \epsilon^{hm}W_{m+p}(x). \quad (4.3)$$

The case $-1 < n < 1$ is similar to the initial conditions with generalized white noise in Burgers turbulence. The energy of the initial signal in such turbulence is determined by the largest cutoff wavenumber, so in our model by the smallest scale p . If $p \rightarrow -\infty$ the energy of the model signal (as the energy of white noise) will tend to infinity. But from the considerations in the previous section we have that at the finite time t all the modes with $t_p < t$ have finite energy $\sim L_p^2/t^2$ due to the nonlinear dissipation, so that the whole energy of the turbulence is also finite. Thus, even in the case of "divergent" initial conditions ($p \rightarrow -\infty$), we will have a "convergent" solution for any time $t > 0$.

The case $n < -1$ is similar to having fractional Brownian motion initial condition in Burgers turbulence. In this case, the series (4.2) diverges and the initial signal $W_p(x)$ is unbounded. But for Burgers turbulence (for the process of particles motion and collisions) only relative velocity of the particles matters. So we can use the same regularisation procedure with $W_p(x)$. Such a procedure was done with the Weierstrass function in [21].

In our case, taking $\varphi_p \equiv 0$, we can introduce the function $W_p^\infty(x) = W_p(x) - W_p(0)$, according to [21], which is finite in all finite spatial intervals. The other way to get a bounded function is to use special phase relations for the modes.

5 Self-similarity properties of deterministic model in one and two dimension

Here we summarise the properties of the evolution of the multiscale deterministic signal using some additional information about scaling characteristics of $W_p(x)$, and compare them with the properties of the Burgers turbulence.

Let us consider the evolution of the multiscale signal

$$v_0(x) = v_p(x) + W_p(x). \quad (5.1)$$

It was shown that at times t for which $t > \tilde{t}_p$, heavy particles with mass $M_p = \rho_0 L_p$ appear and their coordinates are determined by the relation (3.5). These particles collide at time \tilde{t}_{p+1} , ($\tilde{t}_{p+1}/\tilde{t}_p = N^{\frac{n+3}{2}}$, $N = \epsilon^{-1}$), and new particles with masses $m_{p+1} = \rho_0 L_{p+1} = m_p N$ appear. Their motion will be determined by the same law (3.5) with substitution $p \rightarrow p+1$. Using the scaling properties of $W_p(x)$ (4.3) we have, that the motion of the particles in this interval will be similar to the motion of the particles in the interval $[\tilde{t}_p, \tilde{t}_{p+1}]$ if we rescale the time $t/\tilde{t}_p \Rightarrow t/\tilde{t}_{p+1}$. Since the ratio t_{p+1}/t_p does not depend on p , one can speak about the logarithmic periodic self-similarity of the motion of the particles. This means that at arbitrary interval $[\tilde{t}_q, \tilde{t}_{q+1}]$ the motion of the particles will be similar to the motion of the particles in the interval $\tilde{t}_p, \tilde{t}_{p+1}$, by the scaling factor $x_p/x_q = \epsilon^{p-q}$ in space, and the scaling function $t_p/t_q = (\epsilon^{-\frac{n+3}{2}})^{p-q}$ in time. The coordinates and masses of the particles fully

determine the velocity field, and so the solution of Burgers' equation is also logarithmic periodic self-similar.

With each collision, the mass $M(t)$ of the particles increases $N = 1/\epsilon$ times. The time interval between the two successive collisions increases as $t_{p+1}/t_p = N^{\frac{n+3}{2}}$. Thus, by the approximation of piecewise constant function $m(t)$ by the power law

$$m(t) \simeq m_0(t/t_0)^{(n+3)/2}. \quad (5.2)$$

we obtain the same result as for the Burgers turbulence. In our case, m is proportional to the period of the smallest mode at time t , and is analogous to the integral scale in Burgers turbulence.

In the case $n > -1$ we can also estimate the energy decay of the model signal. For $n > -1$ and $\epsilon \ll 1$ the main energy of the signal at time t is in the smallest mode and is proportional to $L^2(t)/t^2$. Thus, we have here again the same law for the energy decay as for Burgers turbulence.

The numerical simulation based on the algorithm [27] was done to illustrate the process of particles merging and velocity field evolution. The trajectories of the particles and profile of the field at different times are plotted for the initial "white noise" signal ($n = 0$, $h = -1/2$) in Fig.3, and for the initial "Brownian" motion ($n = -2$, $h = 1/2$) in Fig.4. Ten modes with the ratio of successive wavenumbers $\epsilon = 1/N = 1/2$ were used. The plots show the initial stage of the evolution in some relatively small region where the finiteness of the number of modes is not significant.

In Fig. 3 one can see that for $n = 0$ the initial "sawtooth" multiscale function oscillates near $v = 0$ like a "white noise" with finite variance. After the collision of light particles, when the reverse sawtooth function transforms into a sawtooth wave with positive gradient $\partial_x v = 1/t$, the structure of the signal is relatively simple, and even for $N = 2$ the main energy remains in the mode with smallest wavenumber.

In the case $n = -2$ the initial profile has a large deviation behaviour which is typical for Brownian motion functions. After merging of light particles, the sawtooth profile has a set of small shocks with different amplitudes, which is also similar to the properties of Brownian signal in the Burgers turbulence [28].

In Figs. 3(c) and 4(c) the velocity field at three successive merger times $t_*/t_{**} = N^{(n+3)/2}$ are plotted. These figures show the logarithmic periodic self-similarity of the evolution of multiscale signals.

We notice now that such multiscale waves may be constructed for multidimensional Burgers' equation. Let us assume that the initial vector field $\mathbf{V}_p(\mathbf{x})$ is an infinite series of "reverse" modes $\mathbf{v}_r(\mathbf{x})$:

$$\mathbf{V}_p(\mathbf{x}) = \sum_{r=p}^{\infty} \mathbf{v}_r(\mathbf{x}), \quad (5.3)$$

In the two dimensional case, the r th "reverse" mode may be composed of piecewise linear functions defined on a system of regular triangles of size L_r covering the plane. We consider here the special case when the ratio of the scales of two adjacent modes is $L_{r+1}/L_r = \epsilon^{-1} = N = 2$. We assume also the special symmetry and phase relation between the different modes. In our case one big triangle is divided into four smaller triangles with vertices

located at midpoints of its sides (see Fig.5). We assume that inside each triangle in the r th mode the velocity has a linear profile $\mathbf{v}_r(\mathbf{x}) = -\gamma_r(\mathbf{x} - \mathbf{x}_+)$, where \mathbf{x}_+ is the coordinate of the center of the triangle. The solution of the multidimensional Burgers equation for such initial perturbation

$$\mathbf{v}(\mathbf{x}, t) = \frac{-\gamma(\mathbf{x} - \mathbf{x}_+)}{1 - \gamma t} \quad (5.4)$$

is now valid inside the triangle of size $L_r(t) = L_r(1 - t\gamma_r)$. The value γ_r^{-1} has the dimension of time, and at the finite time $t_r = \gamma_r^{-1}$ the velocity gradient becomes infinite.

On the other hand, at time $t = t_r$, the mode transforms into a "direct" sawtooth wave with the universal behaviour inside the new set of triangles and with the gradient $1/t$ independent of the amplitude and wavenumber of the mode:

$$\mathbf{v}(\mathbf{x}, t) = \frac{\mathbf{x} - \mathbf{x}_c}{t}, \quad (5.5)$$

where \mathbf{x}_c is now the center of the triangle, coinciding with the top of the initial triangular set. Consider now the evolution of a gas of sticky particles in the case of independent evolution of the r th mode. Then, it is obvious that at the initial stage, inside the "collapsing" triangle of size $L_r(t) = L_r(1 - t\gamma_r)$ the density increases as

$$\rho(\mathbf{x}, t) = \rho_0 \frac{1}{(1 - t/t_p)^2}, \quad (5.6)$$

while ρ is zero outside "collapsing" triangular in each cell. At time $t = t_r$, all the light particles in each cell collide into a single heavy particle with mass

$$m_r = \rho_0 L_r^2 \sqrt{3}/4, \quad (5.7)$$

and the heavy particles' positions are equal to the center of the initial triangle \mathbf{x}_+ .

We assume also that the evolution of the r th mode is characterised by a nonlinear time t_r the same as in the one dimension case (2.4):

$$t_r = \gamma_r^{-1} = t_0 / (2^{-(n+3)/2})^r. \quad (5.8)$$

Let us now consider the evolution of the vector field $\mathbf{V}_p(\mathbf{x})$ (5.3) which is an infinite series of "reverse" modes. The evolution of the vector field is very similar to the evolution of the scalar field (3.1). For the gradient of the initial perturbation $\mathbf{V}_p(\mathbf{x})$ we have the same relation (3.2) as in $1D$. The effective time of nonlinearity of the smallest p th mode in the vector field (5.3), in presence of all large scale modes, is determined by the equation (3.3). Thus, after the time of collision \tilde{t}_p , heavy particles with mass m_p (5.7) appear. Velocities of these particles will be determined by the function $\mathbf{V}_{p+1}(\mathbf{x})$ (5.3), which is a sum of all larger modes, but the number of particle collisions is determined by the next $p + 1$ mode. At time \tilde{t}_{p+1} we have a collision of four heavy particles.

The extrapolation of this particle merger process to next generations is evident by recurrence. The q th collision of heavy particles takes place at time \tilde{t}_{p+q} , (5.8) the masses of these particles at this time are determined by the scale of the $(p+q)$ th mode $m_{p+q} = \rho_0 L_{p+q}^2 \sqrt{3}/4$

(5.7). Here also one can speak about the logarithmic periodic self-similarity of the motion of the particles. This means that at arbitrary interval $[\tilde{t}_q, \tilde{t}_{q+1}]$ the motion of the particles will be similar to the motion of the particles in the interval $\tilde{t}_p, \tilde{t}_{p+1}$, by the scaling factor $x_p/x_q = 2^{(q-p)}$ in space, and the scaling function $t_p/t_q = (2^{\frac{n+3}{2}})^{(p-q)}$ in time.

We used computer simulation for studying two dimensional case; results of the simulation were generated in so called VRML (Virtual Reality Modeling Language), which enables to handle three dimensional figure in different projections. Fig. 6 presents snapshots of this modeling. On the Fig. 6(a) one can see that particles formed by small triangles move towards the center of an embracing triangle; this center in its turn, moves towards the center of the next bigger triangle in the hierarchy; e.t.c. Fig.6(b) gives the side-view of this process.

6 Conclusion

In conclusion, we would like to point out that the evolution of the multiscale signal with the Weierstrass spectrum simulates properties of Burgers turbulence such as self-similarity, conservation of large scale structures and has the same laws of the energy decay and integral scale. The difference between the deterministic model and Burgers turbulence is that here we have the exact solution for the evolution of multiscale signals and these properties are not stochastic but deterministic. The evolution of the multiscale signal is exactly self-similar in logarithmically spaced time intervals. The evolution of the large scale modes is completely independent of the small scales modes, even if these have very large amplitudes.

These properties take place for Burgers turbulence in the stochastical sense and, moreover, for a signal with cutoff frequencies of small scales, only asymptotically. Of course, these properties of the multiscale signal are determined by the special form of modes (reverse sawtooth function), the special relations between wavenumbers of modes ($k_{r+1} = k_r/N$, where N is an integer) and their phase relations.

On the other hand, these model signals do not reflect such properties of Burgers turbulence as qualitative difference in the behaviour of the turbulence for $n < 1$ and $n > 1$ in the power spectrum (1.9) due to the process of generation of large scale components in the spectrum. For the deterministic model this process is not present due to the special relation of wavenumbers.

Let us now move to the mechanical interpretation of solution of the Burgers equation. For the initial reverse sawtooth wave, all the matter turns into heavy particles at the same moment of time. Thus, after this time, the evolution of Burgers turbulence is fully determined by the motion of heavy particles. The trajectories of heavy particles form regular tree-like structure on the plane (X, t) , see Figs. 3 and 4. The properties of this structure depend on the parameters of our model. The integer $\epsilon^{-1} = N$ is the number of trajectories which intersect at one point and form a new branch of our structure. For $\epsilon^{-1} = N = 2$ we, thus, obtain binary tree structure. Changing of the parameter h stretches or contracts the structure in the t direction. One can say that our structure is the plane representation of the N -tree; the root of our tree is located at $t = +\infty$. This tree is similar to the flattened fractal model of botanical umbrella tree (see [21]). If we take some node (X, T) of this

structure as a root, and consider the trajectories of all heavy particles, which will merge at the moment of time T at this point (X, T) we shall also obtain an n -tree. The whole tree seems self-similar, because every branch plus the branches it carries is a reduced scale version of the whole.

We also notice that such multiscale waves may be constructed for multidimensional Burgers' equation.

7 Acknowledgements

The authors are grateful to U. Frisch for useful discussions and for his hospitality at the Observatoire de la Côte d'Azur, to G.M. Molchan, A.I. Saichev, A. Noullez and W.A. Woyczynski for useful discussions. This work was partially supported by the French Ministry of Higher Education, by INTAS through grant No 97-11134, by RFBR through grant 99-02-18354.

References

- [1] J.R. Angilella, J.C. Vassilicos, Spectral, diffusive and convective properties of fractal and spiral fields, *Physica D*, 124 (1998) 23–57.
- [2] E. Aurell, S. Gurbatov, I. Wertgeim, Self-preservation of large-scale structures in Burgers turbulence, *Physics Lett. A* 182 (1993) 104–113.
- [3] M. Avellaneda, W. E, Statistical properties of shocks in Burgers turbulence, *Comm. Math. Phys.* 172 (1995) 13-38.
- [4] M.V. Berry, Z.V. Lewis, On the Weierstrass-Mandelbrot fractal function, *Proc. Roy. Soc. A* 340 (1980) 459–484.
- [5] J.P. Bouchaud, M. Mézard, G. Parisi, Scaling and intermittency in Burgers turbulence, *Phys. Rev. E* 52 (1995) 3656–3674.
- [6] J.M. Burgers, Mathematical examples illustrating relations occurring in the theory of turbulent fluid motion, *Kon. Ned. Akad. Wet. Verh.* 17 (1939) 1–53, (also in: F.T.M. Nieuwstadt, J.A. Steketee (Eds.), *Selected Papers of J.M. Burgers*, Kluwer Academic Publishers, Netherlands (1995) 281–334).
- [7] J.M. Burgers, *The Nonlinear Diffusion Equation*, D. Reidel, Dordrecht, 1974.
- [8] A.-L. Barabasi, H.E. Stanley, *Fractal Concepts in Surface growth*, Cambridge University Press, Cambridge, 1995.
- [9] J.D. Fournier, U. Frisch, L'équation de Burgers déterministe et statistique, *J. Méc. Théor. Appl.* 2, Paris (1983b) 699–750.

- [10] U. Frisch, Turbulence: the Legacy of A.N. Kolmogorov, Cambridge University Press, 1995.
- [11] J.L. Gilson, I. Daumont, T. Dombre, A two-fluid picture of intermittency in shell-models of turbulence, in: U. Frisch (Ed.), Advances in Turbulence VII, Kluwer Academic Publishers, Netherlands (1998) 219-222.
- [12] S.N. Gurbatov, D.B. Crighton, The nonlinear decay of complex signals in dissipative media, Chaos 5(3) (1995) 524–530.
- [13] S.N. Gurbatov, A.N. Malakhov, A.I. Saichev, Nonlinear Random Waves and Turbulence in Nondispersive media: Waves, Rays, Particles, Manchester University Press, Manchester, 1991.
- [14] S.N. Gurbatov, A.I. Saichev, Inertial nonlinearity and chaotic motion of particle flux, Chaos 3 (1993) 333–358.
- [15] S.N. Gurbatov, A.I. Saichev, S.F. Shandarin, The large-scale structure of the Universe in the frame of the model equation of non-linear diffusion, Month. Not. Roy. Astr. Soc. 236 (1989) 385–402.
- [16] S.N. Gurbatov, S.I. Simdyankin, E. Aurell, U. Frisch, G. Toth, On the decay of Burgers turbulence, J. Fluid Mech. 344 (1997) 339-374.
- [17] S.N. Gurbatov, G.V. Pasmanik, Self-preservation of large-scale structures in nonlinear viscous medium described by the Burgers equation, J.Exp.Theor.Phys. 88, N.2 (1999) 309–319.
- [18] E. Hopf, The partial differential equation $u_t + uu_x = u_{xx}$, Comm. Pure Appl. Mech. 3 (1950) 201–230.
- [19] L. Kadanoff, A cascade model of turbulence, in: U. Frisch (Ed.), Advances in Turbulence VII, Kluwer Academic Publishers, Netherlands (1998) 201-202.
- [20] S. Kida, Asymptotic properties of Burgers turbulence, J. Fluid Mech. 93 (1979) 337–377.
- [21] Benoit B. Mandelbrot, The fractal geometry of nature, Freeman, New York, 1982.
- [22] G.M. Molchan, Burgers equation with self-similar Gaussian initial data: tail probabilities, J. Stat. Phys. 88 (1997) 1139-1150.
- [23] R. Ryen, Large-deviation analysis of Burgers turbulence with white-noise initial data, Comm. Pure Appl. Math. L1 (1998) 47–75.
- [24] O. Rudenko, S. Soluyan, Theoretical foundation of Nonlinear Acoustics, Plenum, New-York, 1997.

- [25] S.F. Shandarin, Ya.B. Zeldovich, The large-scale structure of the Universe: turbulence, intermittency, structures in a self-gravitating medium, *Rev. Mod. Phys.* 61 (1989) 185–220.
- [26] Ya.G. Sinai, Statistics of shocks in solutions of inviscid Burgers equation, *Commun. Math. Phys.* 148 (1992)601–622 .
- [27] A. Trousov, Linear time algorithms for discrete Legendre transform and for the numerical simulation of Burgers' equation, *Comp. Seism.* 29 (1996) 45-53 (In Russian).
- [28] M. Vergassola, B. Dubrulle, U. Frisch, A. Noullez, Burgers' equation, Devil's staircases and the mass distribution for large-scale structures, *Astron. Astrophys.* 289 (1994) 325–356.
- [29] G.B. Whitham, *Linear and Nonlinear Waves*, Wiley, New York, 1974.
- [30] W.A. Woyczynski, *Burgers–KPZ Turbulence*, Springer-Verlag, Berlin, 1998.

Figure captions

Figure 1: Evolution of one-mode pulse. (a) particle trajectories; (b) evolution of the initial velocity field given in the same spatio-temporal scale. Bold lines on the time axis denote moments at which the profiles of the velocity are plotted.

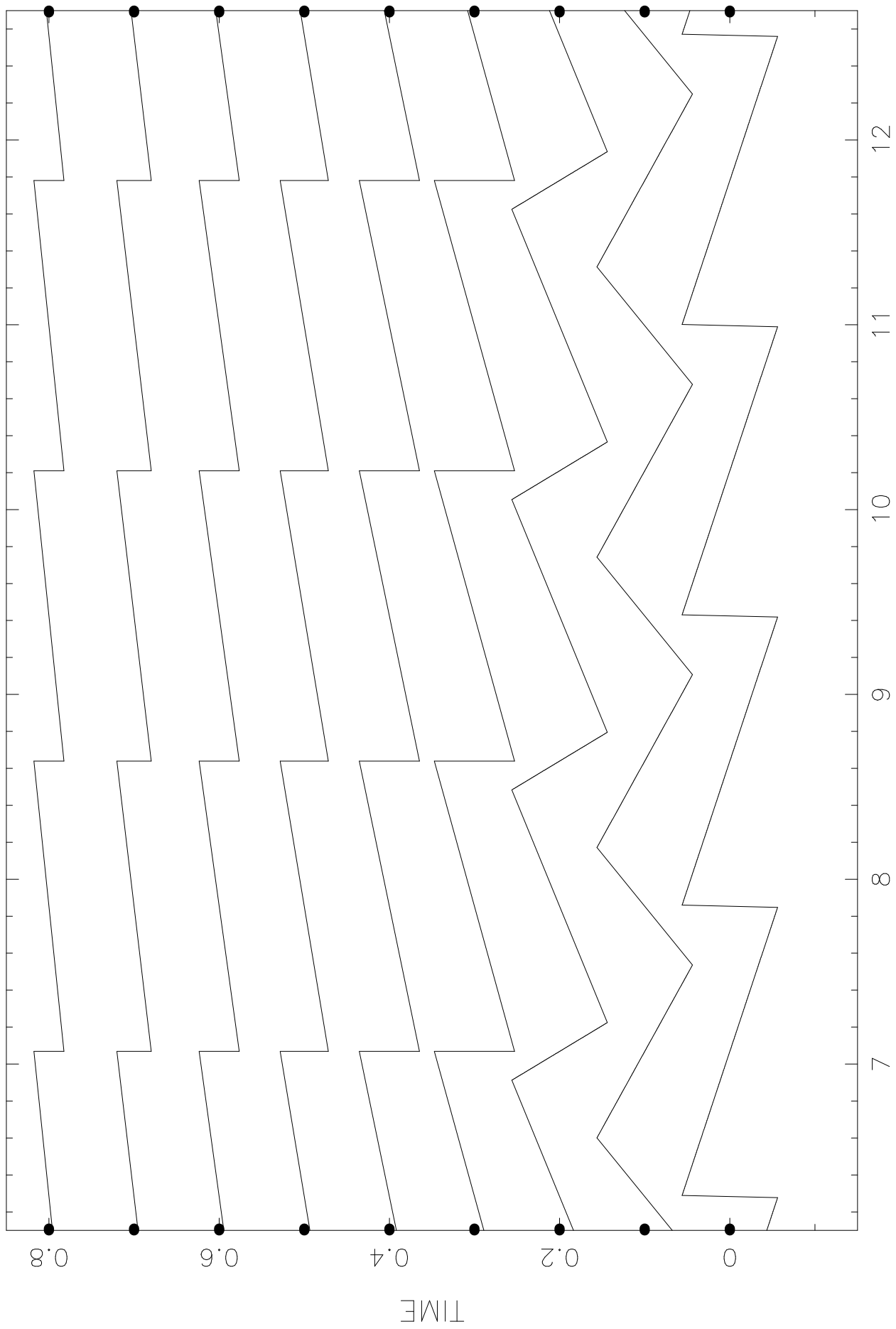
Figure 2: Evolution and interaction of two modes. (a) particle trajectories; (b) evolution of the initial velocity field given in the same spatio-temporal scale. Bold points on the time axis denote moments at which the profiles of the velocity are plotted.

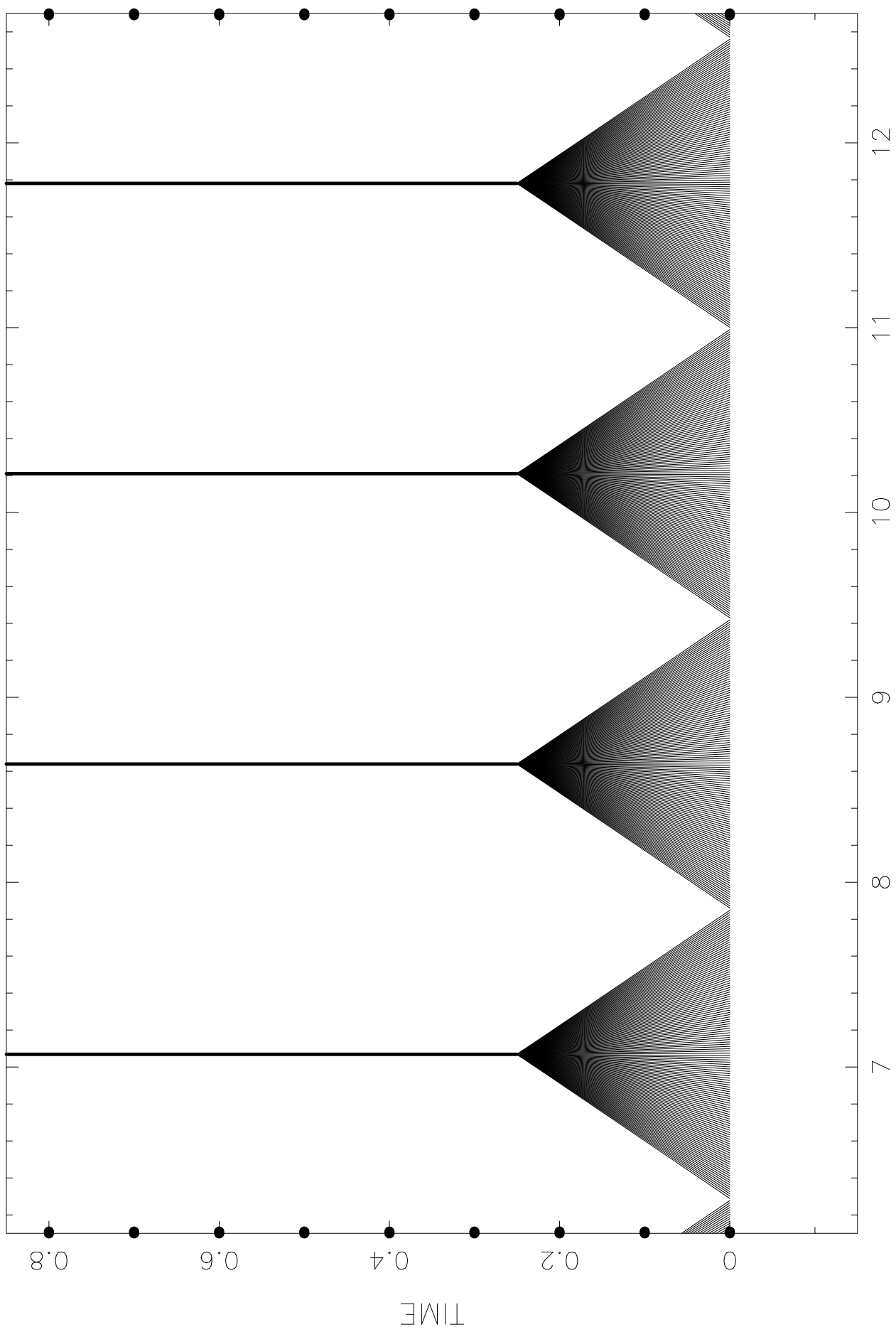
Figure 3: Evolution of the multiscale fractal signal with $n = 0$ ($h = -1/2$), corresponding to "white noise" signal. (a) particle trajectories; (b) evolution of the initial velocity field; (b) velocity field taken at the initial moment of time and then at three successive time moments of self-similarity.

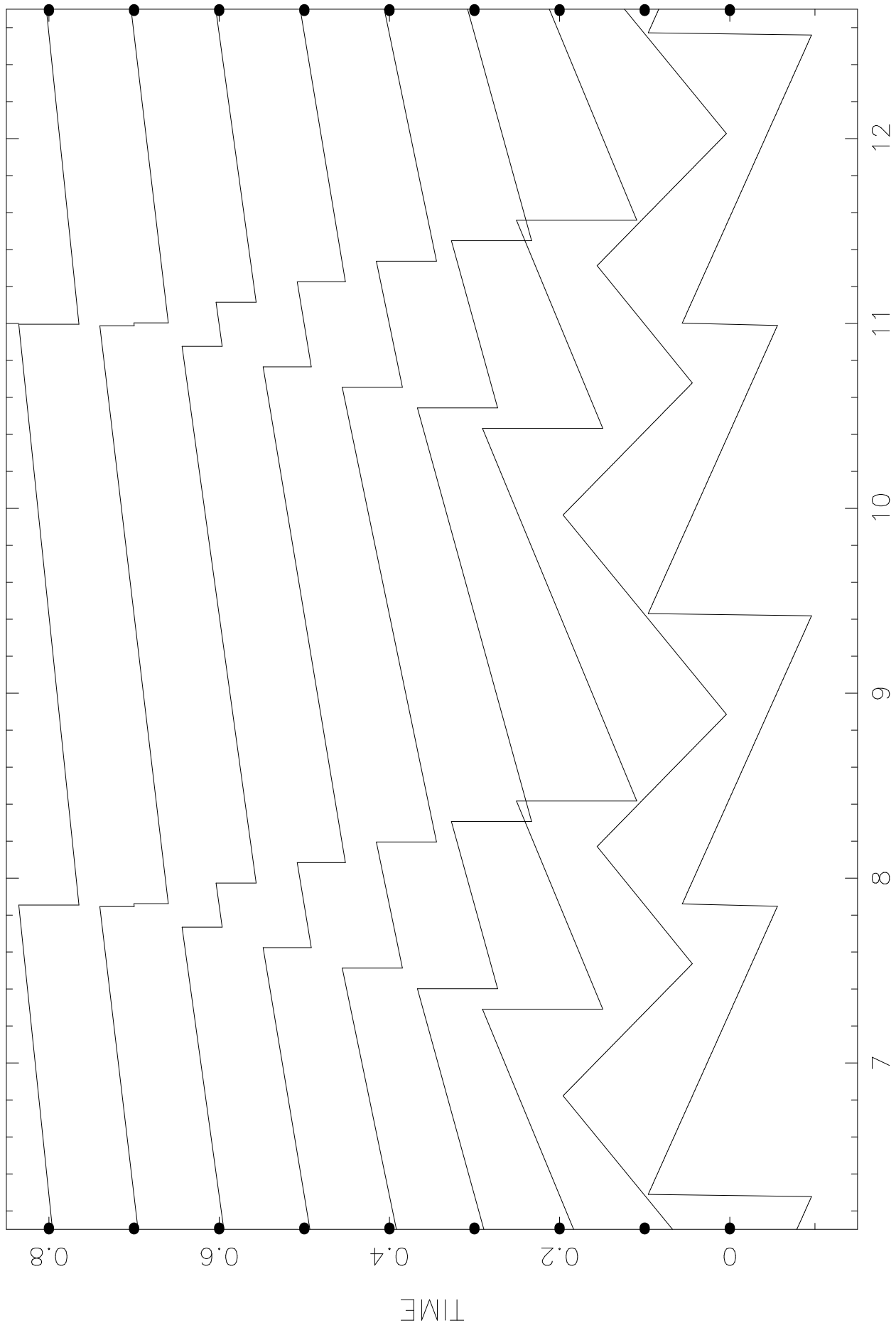
Figure 4: Evolution of the multiscale fractal signal with $n = -2$ ($h = 1/2$), corresponding to "Brownian motion" signal. (a) particle trajectories; (b) evolution of the initial velocity field; (b) velocity field taken at the initial moment of time and then at three successive time moments of self-similarity.

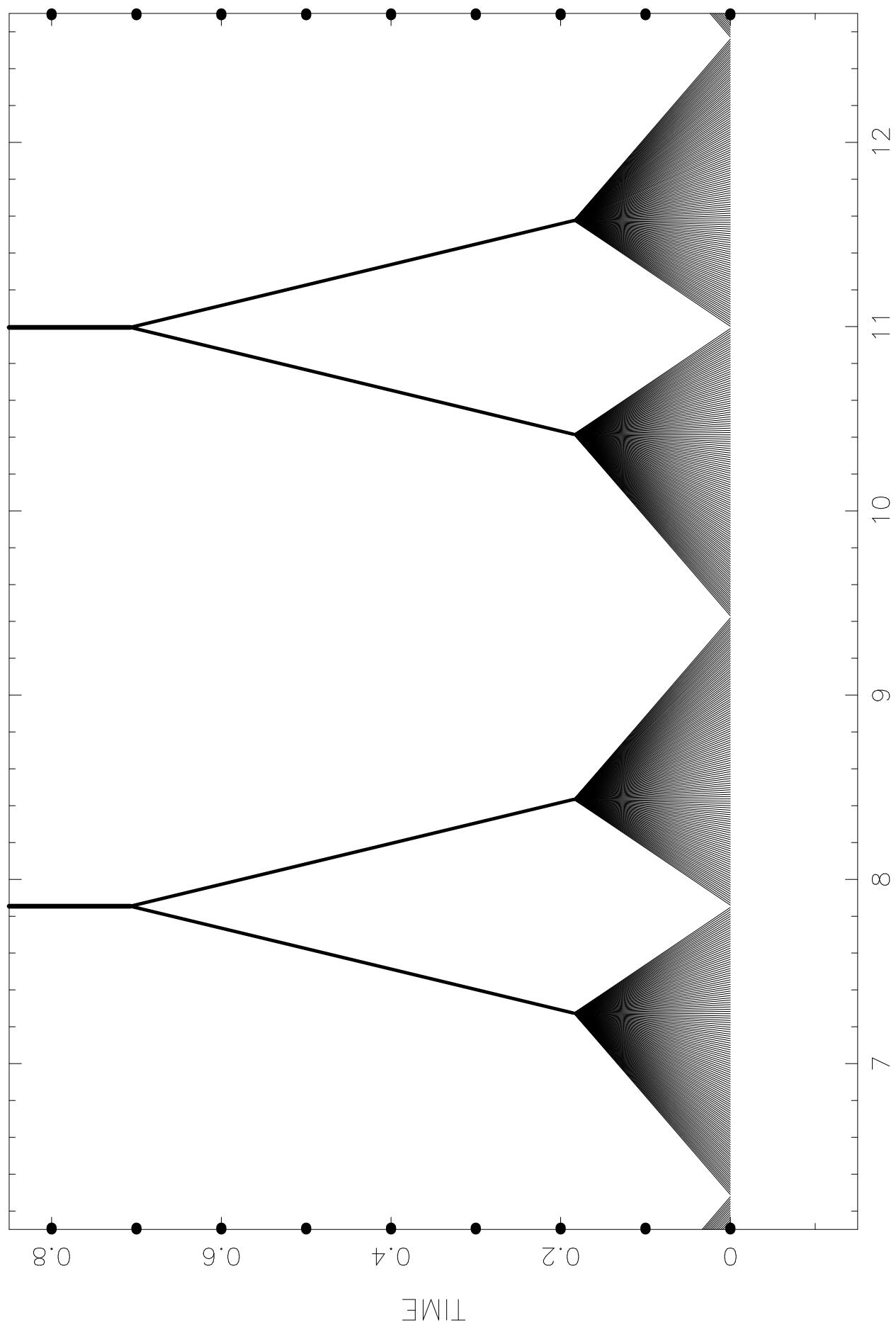
Figure 5: Plane construction for two dimensional case. The hierarchy of triangles, used for the construction of the multiscale signal, with four layers shown. The initial signal is constructed as a series of signals piece-wise linear on triangles.

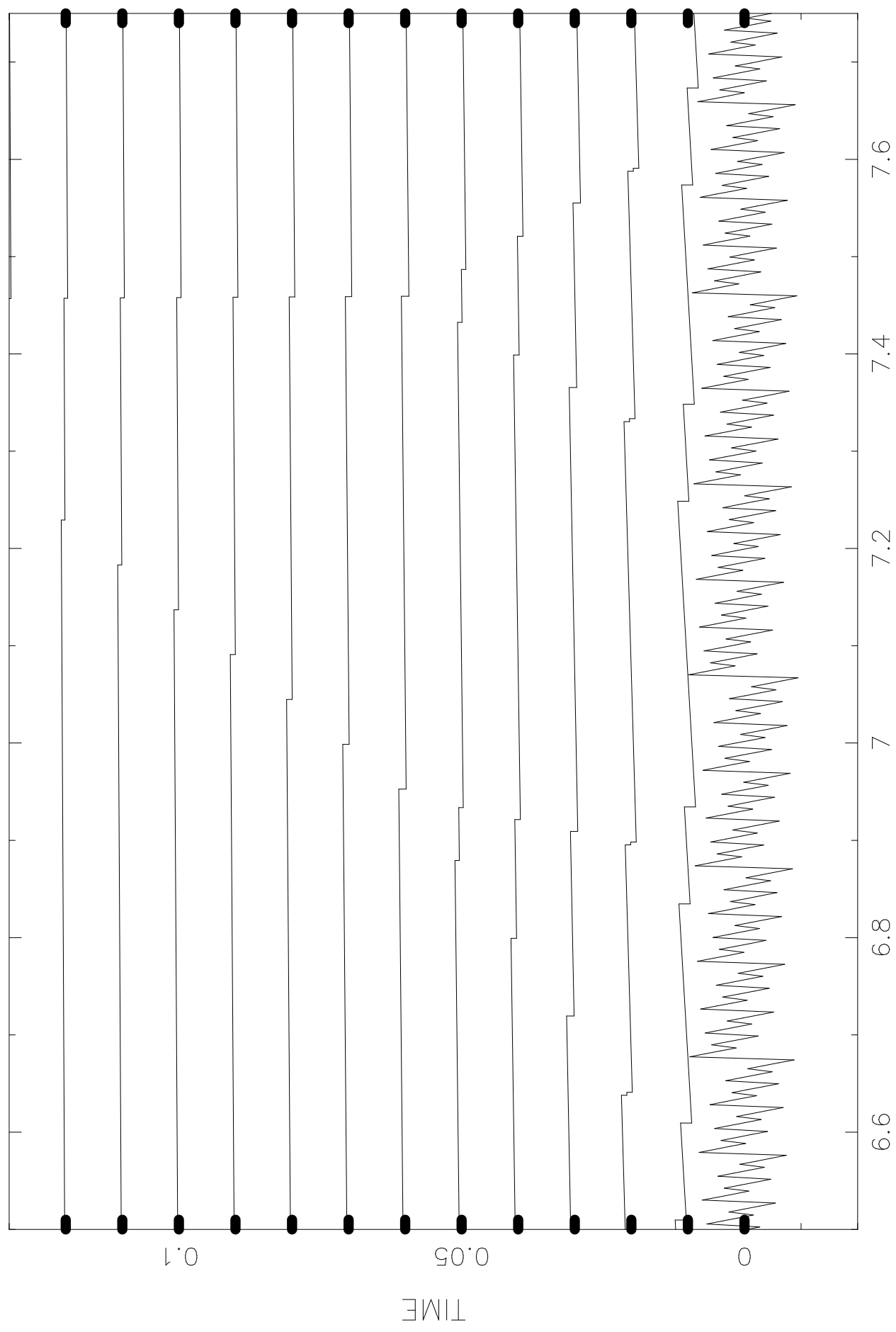
Figure 6: Particle trajectories for the multiscale fractal signal in two dimensional case presented in spatio-time three dimensional space; the width of particle trajectory reflects its mass: (a) top view; (b) side-view.

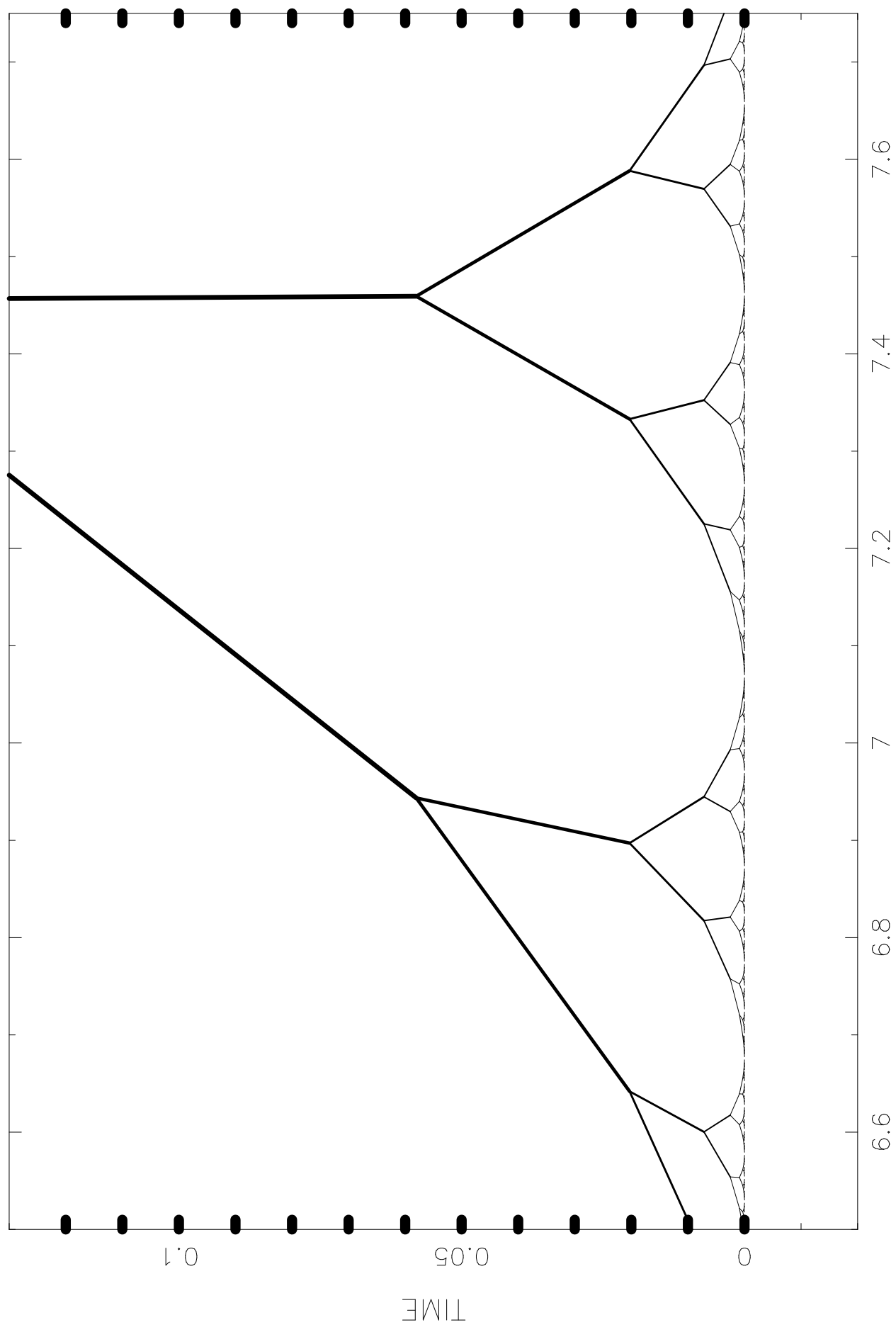






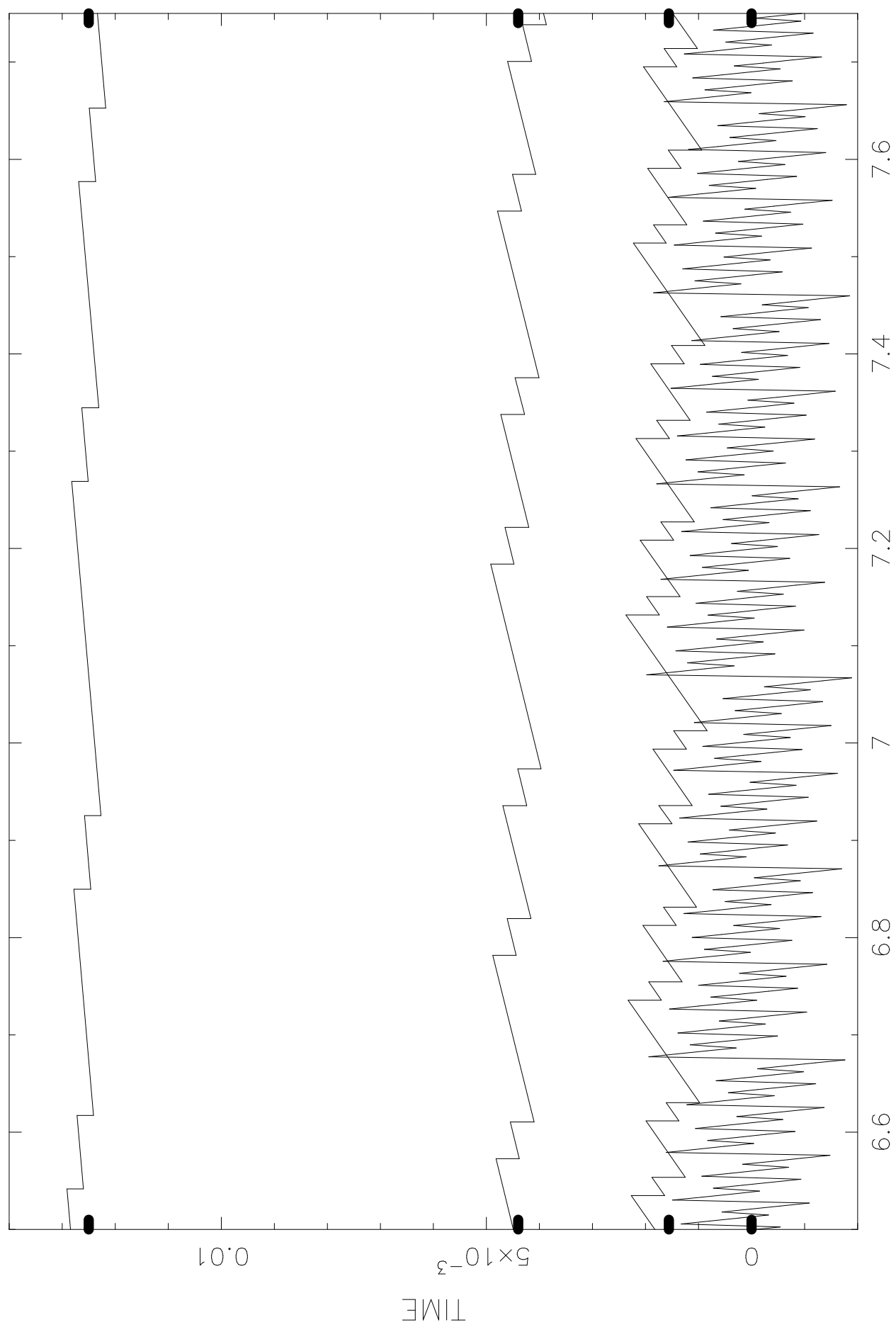






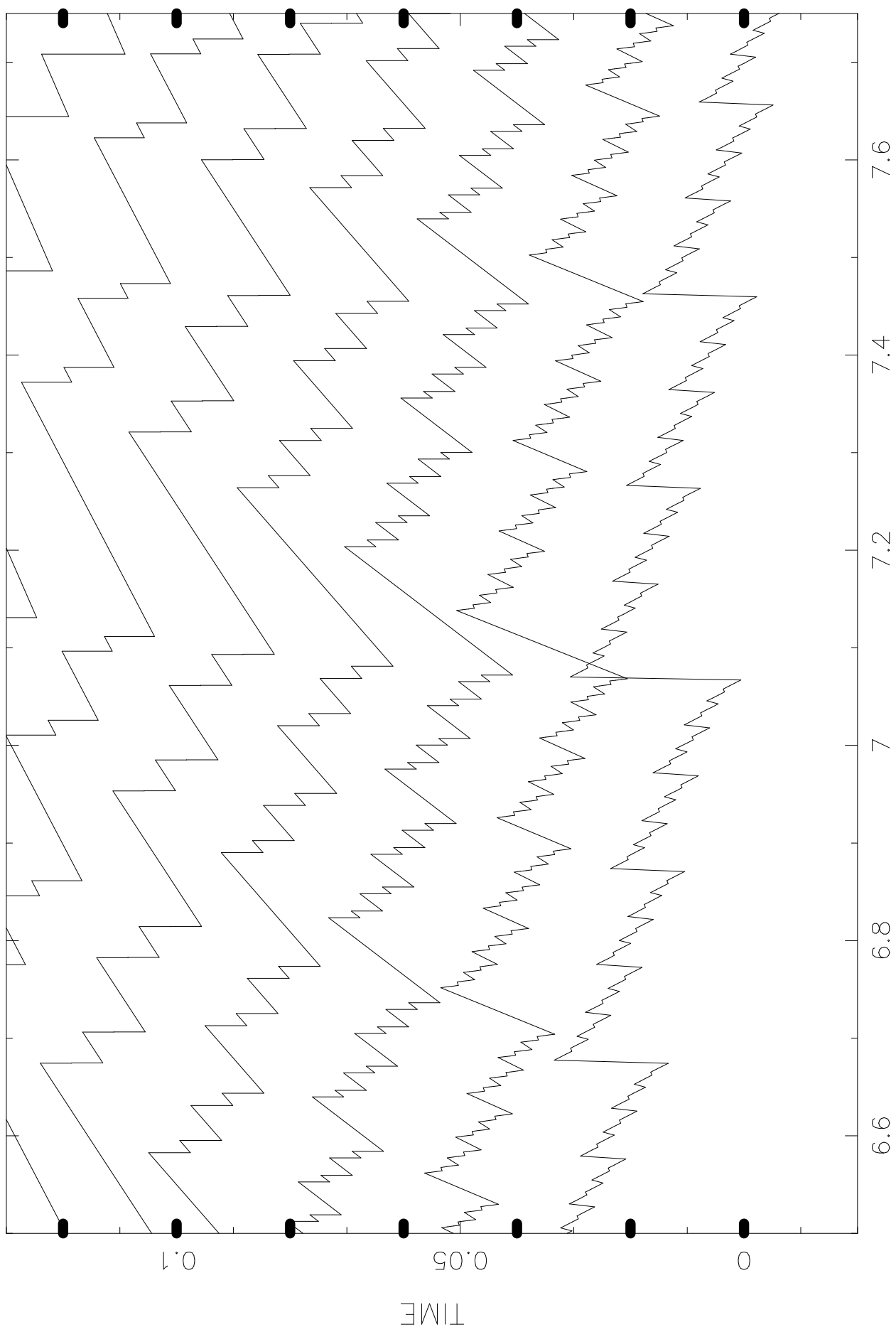
SPACE COORDINATE

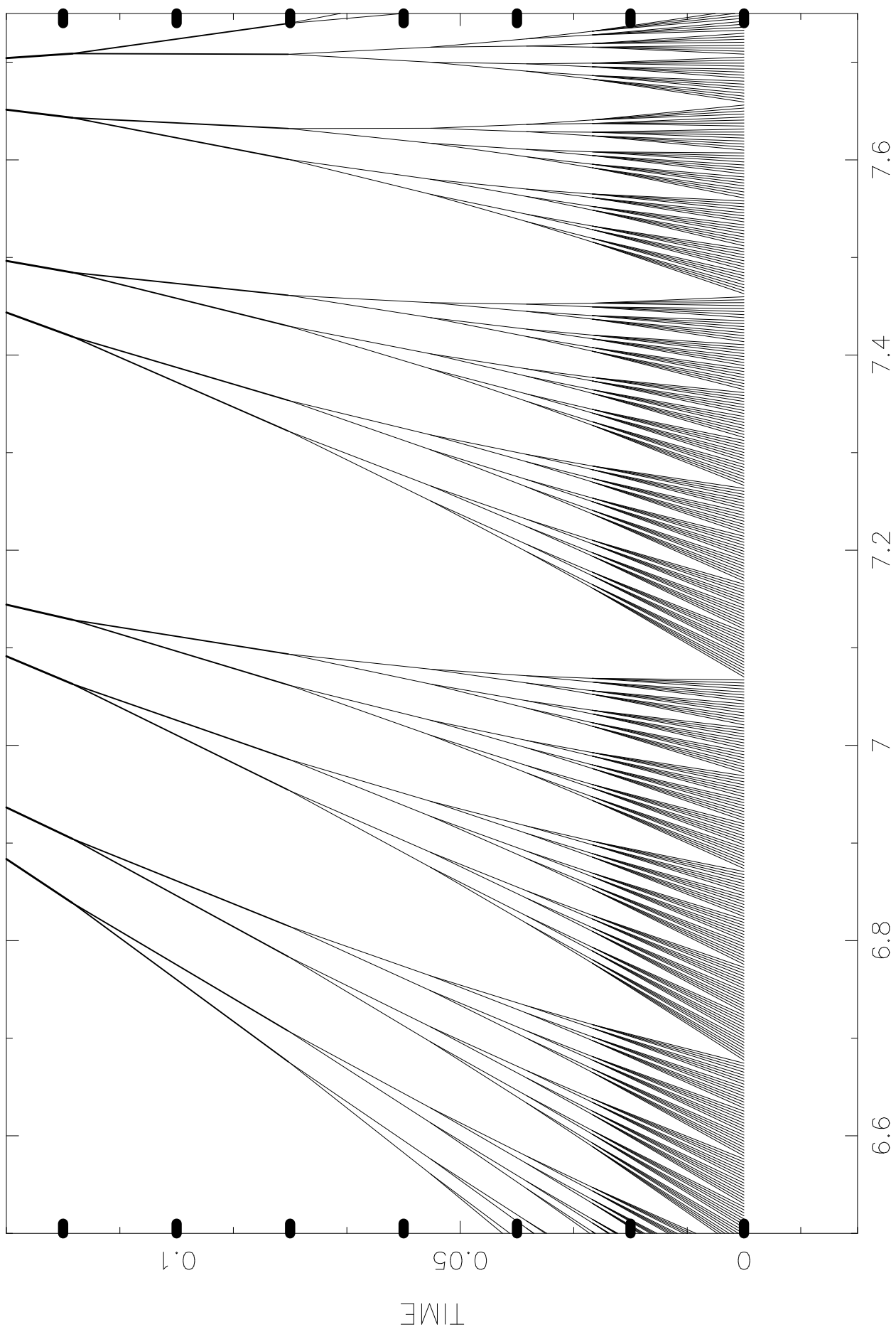
TIME

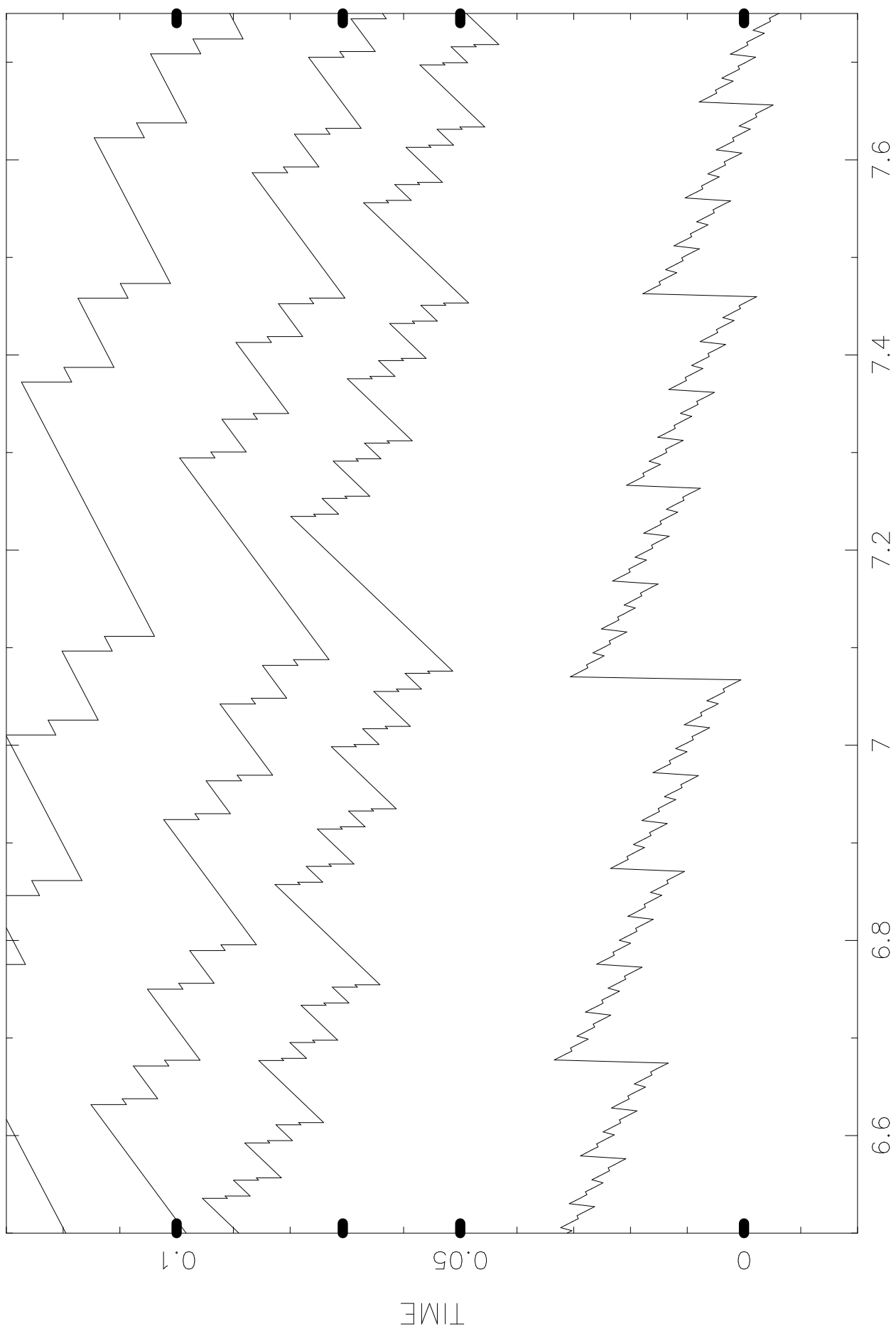


SPACE COORDINATE

TIME







SPACE COORDINATE

TIME

This figure "Fig5.jpg" is available in "jpg" format from:

<http://arxiv.org/ps/physics/0002043v1>

This figure "Fig6a.jpg" is available in "jpg" format from:

<http://arxiv.org/ps/physics/0002043v1>

This figure "Fig6b.jpg" is available in "jpg" format from:

<http://arxiv.org/ps/physics/0002043v1>